

RESEARCH ARTICLE



ISSN: 2321-7758

STEADY STATE AND DYNAMIC RESPONSE FOR BIDIRECTIONAL BUCK–BOOST CASCADE INVERTER

KURATI RAJENDRA SIMHA¹, AKUMALLA KASIM VALI²

¹PG-Student, Dept. of EEE, NOVA COLLEGE OF ENGINEERING & TECHNOLOGY, VIJAYAWADA, India

²Assistant Professor, Dept. of EEE, NOVA COLLEGE OF ENGINEERING & TECHNOLOGY, VIJAYAWADA, India

Article Received: 20/11/2014

Article Revised on: 10/12/2014

Article Accepted on: 17/12/2014



KURATI RAJENDRA SIMHA



AKUMALLA KASIM VALI

ABSTRACT

This paper proposes a bidirectional buck–boost cascade inverter and presents its modelling and control methods. The proposed inverter can be seen as the cascade of a buck converter and a boost converter, both with bipolar outputs. The main inductor current is maintained by buck stage and the output voltage that is to track a given reference is controlled by boost stage. Then, the averaged model for control is given and thereby the buck–boost capability is proven. Utilizing the feed forward compensation technique, a decoupled control scheme is designed afterward. A new modulation strategy is also proposed to minimize the dead time effect. Bidirectional operation with bipolar buck–boost output voltage; reduced output distortion due to advanced modulation minimizing the dead time effect; reduced size and weight with only one main energy storage component; decoupled linear controller design; and good steady-state and dynamic performance including wide operation range, strong robustness to load and input voltage variations, fast dynamic response, and excellent overload protection.

Key Words: - Bidirectional converter, buck–boost cascade converter, control system, inverter, modelling Fuzzy logic controller.

©KY Publications

INTRODUCTION

Nowadays dc–ac inverters have been widely used in various commercial and industrial areas such as motor driving, energy storage, renewable energy generation, etc. The conventional voltage source inverter (VSI) (also referred to as the buck inverter) has taken a very large market share in these applications. It is used in many distinct industrial and commercial applications. Among these applications, uninterruptible power supply (UPS) and ac motor drives are the most important.

One of the characteristics of the buck inverter is that the instantaneous average output voltage is always lower than the input dc voltage. As a consequence, when an output voltage larger than the input one is needed, a boost dc–dc converter must be used between the dc source and inverter. Depending on the power and voltage levels involved, this solution can result in high volume, weight, cost, and reduced efficiency. In this paper, a new VSI is proposed, referred to as boost inverter, which naturally generates an output ac voltage low error larger than

the input dc voltage depending on the duty cycle. Inheriting the characteristics of the buck converter, the VSI can only produce an output voltage lower than its dc input. However, in some applications, e.g., motor driving in electric vehicle systems [1]–[3] and grid-connected fuel cell or photovoltaic systems [4]–[6], both the step-down (buck) and step-up (boost) operations are required. Sometimes, the bidirectional power handling capability of the inverter is also desired in order to recover energy or adapt for back-to-back applications in a wind power system [7]. Therefore, it is necessary to explore an alternative topology that can meet both of the two requirements. Probably, the most natural solution is to use a boost +VSI topology [8], [9]. Although the principle is straight forward, it requires two main energy storage components (i.e., a main inductor and a main capacitor) that will increase the volume, weight, and cost of the system. Also, the control of the boost stage is not as easy as that in ordinary dc–dc applications because of rapid and substantial variations of the load power in ac applications. An alternative to this is the recently developed Z-source converter that combines functionality of the boost and VSI into a single stage [10], [11]. Compared to the boost+VSI scheme, it has higher efficiency due to its compact structure, less harmonics thanks to its second-order filtering network and less distortion since dead time is not needed [10], [12]. Another representative solution is based on the idea of differentiating the outputs of two bidirectional, unipolar dc–ac inverters [9]. The boost or Cuk topology of the two inverter n stages enables a higher output voltage than the input while the differential output allows a lower output voltage and eliminates the dc bias of each inverter stage as well. For this topology, conventional control based on a liberalized model is no longer valid because of large variation of the operation point in ac applications.

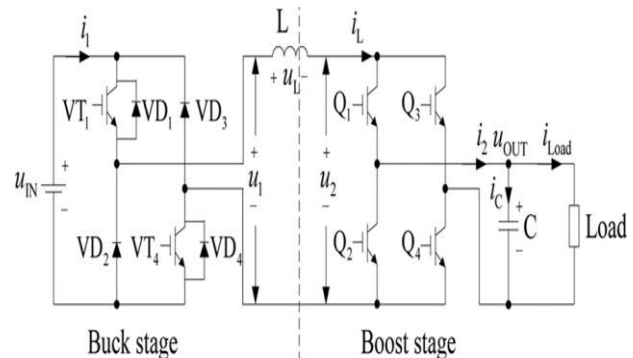


Fig. 1. System topology of the bidirectional buck–boost cascade inverter

In fact, finding a bidirectional converter with buck–boost capabilities has long been discussed in developing the dc–dc converters. For dc–dc power conversion, to handle the bidirectional power flow, one only need to replace the diodes in the classic step-up/down circuits, e.g., buck–boost, Cuk, buck–boost cascade circuits, etc., with bidirectional current switches. However, since these bidirectional converters cannot produce a bipolar output, seldom efforts are devoted to adapt them for dc–ac conversions. Besides the bipolar output issue, to extend them to inverters, the control complexity should also be considered seriously.

Among these topologies, the buck–boost cascade converter is most advantageous in control since it has two control freedoms. For dc–dc applications, this advantage is not so remarkable and even offset by the cost on additional devices to a large extent. However, for dc–ac applications, this additional control freedom can be very favourable. Therefore, with special consideration on the control superiority, an inverter that successfully extends the functionality of a bidirectional buck–boost cascade dc–dc converter is proposed. This paper is organized as follows. First, the operation principle of the proposed inverter is explained. Then, the switching function model of the inverter is established with detailed analysis.

II. SYSTEM ANALYSIS AND MODELING

The topology of the proposed inverter is shown in Fig. 1. The overall system can be seen as the cascade of a buck converter and a boost converter, both with bipolar outputs, which are referred to as the buck stage and the boost stage,

respectively, throughout this paper. $Q_1 - Q_4$ is unidirectional devices such as reverse blocking insulated gate bipolar transistors (IGBTs) or ordinary IGBTs with a blocking diode. i_1 and u_1 are the input current and output voltage of the buck stage while u_2 and i_2 are the input voltage and output current of the boost stage, respectively. u_1 is the voltage across the main inductor L and i_c is the input current of the output capacitor C . Note that all of the electric variables in this figure represent their instantaneous value and their direction denotes the selected sign convention. In conventional control for a buck–boost cascade converter, only one of the two stages is activated while the other is kept feed through, i.e., the converter assumes either the buck or the boost topology. Besides the existing characteristics of the two topologies, this simple combination does not bring about any new features. However, in the proposed control scheme, the system is operating under continuous conduct mode and both of the two stages are activated: the buck stage maintains the main inductor current constant while the boost stage regulates the output voltage to follow the given command. With this control strategy, the control freedom of the buck–boost cascade converter is increased, and therefore, simpler controllers and improved performance can be obtained, as discussed in detail in the following sections.

A. Operation of the Buck Stage

During normal operation, the inductor current is kept at a positive value by the buck stage. Hence, there are only four conducting patterns for the buck stage, as shown in Fig. 2(a)–(d) (the arrow denotes the actual current direction). In the positive bucking phase (a), VT_1 and VT_4 are conducting and the energy is transferred from the battery to the inductor as well

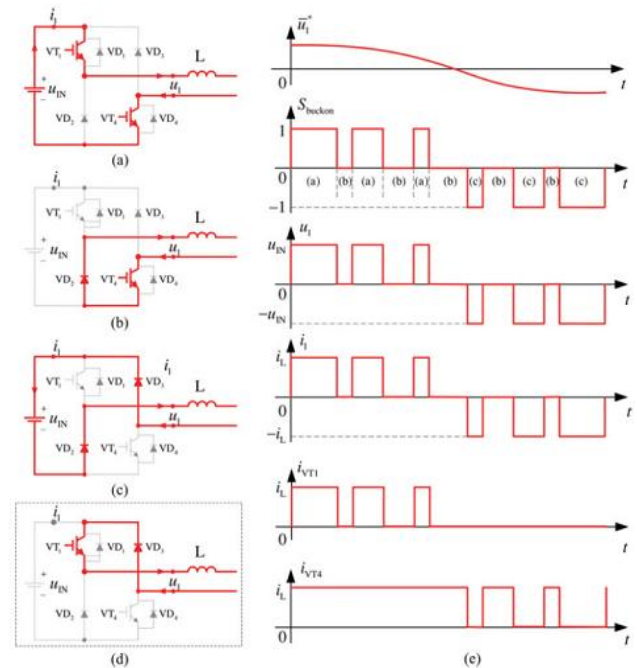


Fig. 2. Conducting patterns and illustrative waveforms of the buck stage. (a) Positive bucking. (b) Free-wheeling (c) Negative bucking. (d) Free-wheeling(Unused). (e) Illustrative waveforms.

Ignoring the forward voltage of the semiconductor devices, then the relations $u_1 = u_{IN}$ and $i_1 = i_L$ hold. In the freewheeling phase (b) or (d), VD_2 and VT_4 (or VD_3 and VT_1) are conducting and the energy is transferred from the inductor to the boost stage, so $u_1 = 0$ and $i_1 = 0$. Note that phases (b) and (d) are equivalent and only (b) is used in the following discussion and design. In the negative bucking phase (c), VD_2 and VD_3 are conducting and the energy is transferred from the inductor and boost stage to the battery, so $u_1 = -u_{IN}$ and $i_1 = -i_L$.

Accordingly, a bipolar voltage output can be obtained. In positive bucking and freewheeling phases. $u_1 = S_{VT_{1ON}} u_{IN}$ and $i_1 = S_{VT_{1ON}} i_L$. If a negative $\overline{u_1}$ is desired, it will switch between the negative bucking and freewheeling phases. In this situation, these are $u_1 = -S_{VD_{3ON}} u_{IN}$ and $i_1 = -S_{VD_{3ON}} i_L$. Here, $S_{VT_{1ON}}$ and $S_{VD_{3ON}}$ are the switching functions of VT_1 and VD_3

$$S_{VT_1(VD_3)ON} = \begin{cases} 1, \text{ when } VT_1(VD_3) \text{ is ON} \\ 0, \text{ when } VT_1(VD_3) \text{ is OFF} \end{cases} \quad (1)$$

Switching functions of the buck stage

$$S_{buckON} = \begin{cases} S_{VT_1ON} & \text{when } \bar{u}_1^* \geq 0 \\ -S_{VD_3ON} & \text{when } \bar{u}_1^* < 0 \end{cases} \quad (2)$$

$$\begin{cases} u_1 = S_{buckON} u_{IN} \\ i_1 = S_{buckON} i_L \end{cases} \quad (3)$$

B. Operation of the Boost Stage

Similarly, since the inductor current i_L is positive, there are four main conducting patterns for the boost stage as shown in Fig. 3 (the commutation transients are not included).

In the positive boosting phase (a), Q1 and Q4 are conducting and the energy is transferred from the source of the boost stage (i.e., the buck stage) as well as the inductor to the load, so $i_2 = i_L$ and $u_2 = u_{OUT}$. In the charging phase (b) or (d), one of the bridge legs is conducting (e.g., Q1 and Q2) and the energy is transferred from the buck stage to the inductor, so $i_2 = 0$ and $u_2 = 0$. The case for the negative boosting phase (c) is similar to phase (a) except that the output polarity is negative, so $i_2 = -i_L$ and $u_2 = -u_{OUT}$.

If a positive averaged output current \bar{i}_2 is desired, in this situation, $i_2 = S_{Q_2OFF} i_L$ and $u_2 = S_{Q_2OFF} u_{OUT}$. If a negative \bar{i}_2 is desired, it will switch between the negative boosting and charging phases. In this situation, $i_2 = -S_{Q_4OFF} i_L$ and $u_2 = -S_{Q_4OFF} u_{OUT}$. Here, S_{Q_2OFF} and S_{Q_4OFF} are the switching functions of Q2 and Q4 is

$$S_{Q_2(Q_4)OFF} = \begin{cases} 1, \text{ when } Q_2(Q_4) \text{ is OFF} \\ 0, \text{ when } Q_2(Q_4) \text{ is ON} \end{cases} \quad (4)$$

Switching functions of the boost stage

$$S_{boostOFF} = \begin{cases} S_{Q_2OFF}, \text{ when } \bar{i}_2^* \geq 0 \\ -S_{Q_4OFF}, \text{ when } \bar{i}_2^* < 0 \end{cases} \quad (5)$$

$$\begin{cases} i_2 = S_{boostOFF} i_L \\ u_2 = S_{boostOFF} u_{OUT} \end{cases} \quad (6)$$

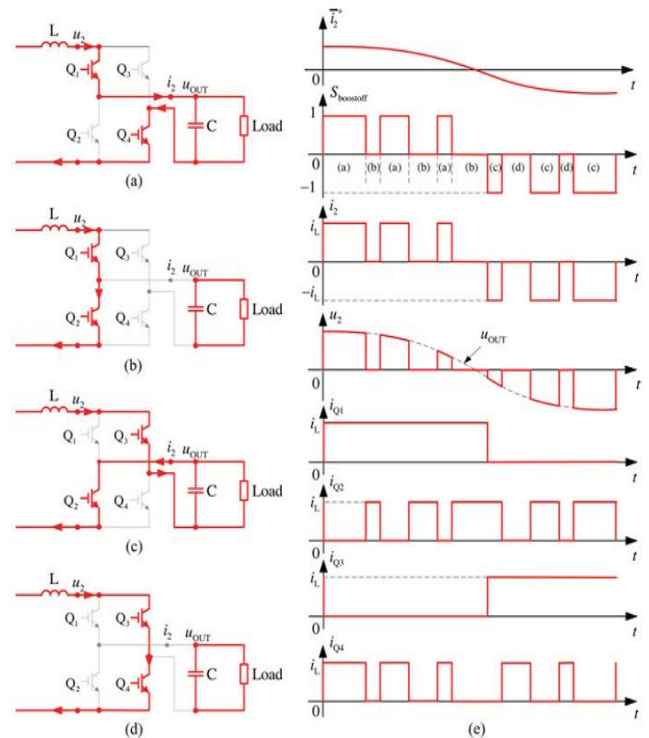


Fig. 3. Conducting patterns and illustrative waveforms of the boost stage. (a) Positive Boosting. (b) Charging (c) Negative Boosting. (d) Charging. (e) Illustrative Waveforms.

Therefore, a bipolar current output can be obtained.

III. SYSTEM CONTROL

A. Averaged Model for Control

For the sake of control, a locally averaged model is often necessary. Based on the switching function model, averaged model can be easily obtained

$$\begin{cases} \frac{d\bar{i}_L}{dt} = \frac{1}{L} (D_{buckON} \bar{u}_{IN} - D_{boostOFF} \bar{u}_{OUT}) \\ \frac{d\bar{u}_{OUT}}{dt} = \frac{1}{C} (D_{boostOFF} \bar{i}_L - \bar{i}_{Load}) \end{cases} \quad (7)$$

where the duty cycles D_{buckON} and $D_{boostOFF}$ are the local average of S_{buckON} and $S_{boostOFF}$, respectively. As previously mentioned during normal operation, the inductor current \bar{i}_L is kept constant.

Therefore, let $\frac{di_L}{dt} = 0$; from the first equation in (8),

it can be found that

$$\overline{u_{OUT}} = \frac{D_{buckON}}{D_{boostOFF}} \overline{u_{IN}} \tag{8}$$

Since $|D_{buckON}|, |D_{boostOFF}| \in [0,1]$, this equation effectively proves the buck/boost capability of the proposed system. The overall control strategy can be divided into two parts: the buck stage controls the current loop whereas the boost stage controls the voltage loop.

B. Current Loop Design

The control objective of the buck stage is to regulate the main inductor current to a positive value i_L^* . From (7), in order to eliminate the disturbances from the battery input and the boost stage, a feed forward compensator can be designed.

$$D_{buckON}^* = \frac{u_L^* + D_{boostOFF}^* \overline{u_{OUT}}}{\overline{u_{IN}}} \tag{9}$$

Where D_{buckON}^* and D_{boost}^* are the duty cycle commands for the buck stage and boost stage, respectively. u_L^* is the voltage reference for the main inductor, normally given by the current controller. After this compensation, the current channel simply becomes an integrator

$$\frac{di_L}{dt} = \frac{1}{L} u_L^* \tag{10}$$

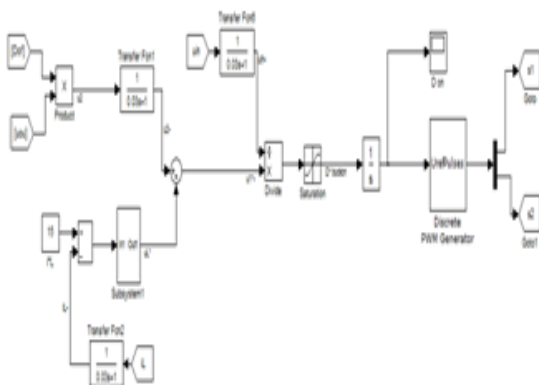


Fig.4. Control scheme of the current loop.

In order to eliminate the errors caused by parasitic parameters and switching operation, a conventional proportional-integral (PI) controller

can be used to complete the current loop. The current control scheme is shown in Fig. 3, where T_s in the filter block is the switching cycle. The equivalent modulation block is constructed according to (2). However, the sign of the equation 1

$D_{buckON}^* = \frac{u_1^*}{u_{IN}}$ is utilized instead of the variable

u_1^* to determine the value of S_{buckON} . This is simply because $\overline{u_{IN}}$ is always positive. The actual implementation of the modulation block that generates the gate pulses for the switching devices will be given later.

C. Voltage Loop Design

The control objective of the boost stage is to control the output voltage to follow the reference u_{OUT}^* . In order to eliminate the disturbances from the load and the buck stage, a feed forward compensator can be designed

$$D_{boostOFF}^* = \frac{i_C^* + \overline{i_{Load}}}{i_L} \tag{11}$$

Where i_C^* is the current reference for the output capacitor, normally given by the voltage controller. Similar to the current loop, after this compensation, the voltage channel becomes an integrator

$$\frac{du_{OUT}}{dt} = \frac{1}{C} i_C^* \tag{12}$$

As a good starting point for most of the industrial applications, a simple PI controller can be applied to complete the voltage loop. The voltage control scheme is shown in Fig. 4. Note that the load current compensation can improve the dynamic response of the system under load variation, but it is not indispensable in this scheme. For low-cost applications, this compensation module can be removed without modifying other parts of the design. In these cases, the load disturbance will be totally rejected by the PI controller, i.e., the output of the PI directly gives the reference for i_2^* . For high-performance applications, a PI controller cannot guarantee a perfect tracking in the case of a periodic reference, according to the internal model principle. In these cases, the PI controller in Fig. 4 can readily be replaced by advanced controllers such as

repetitive controller or deadbeat controller, etc. The equivalent modulation block is constructed according to (5). However, the sign of the equation

$$D_{boostOFF}^* = \frac{\bar{i}_L}{i_L^*}$$

to determine the value of $S_{boostOFF}$.

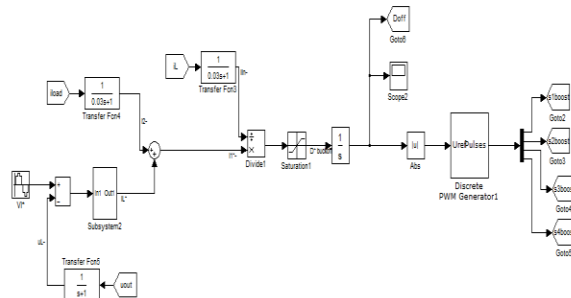


Fig.5 Control scheme of the voltage loop.

IV. SIMULATION RESULTS

In order to validate the proposed bidirectional buck–boost cascade inverter and its control scheme, a prototype system of 500 W has been simulated and implemented.

1) Resistive Load:

As the typical test for inverters, a resistive load ($R_{Load} = 110 \text{ Ohm}$) is connected to the output of the inverter. With 96-V dc input, the inverter is commanded to generate a 220 Vrms/50Hz ac output. Simulation results are summarized in Fig.6. From (a), it can be seen that i_L is successfully regulated at 15 A by the buck stage.

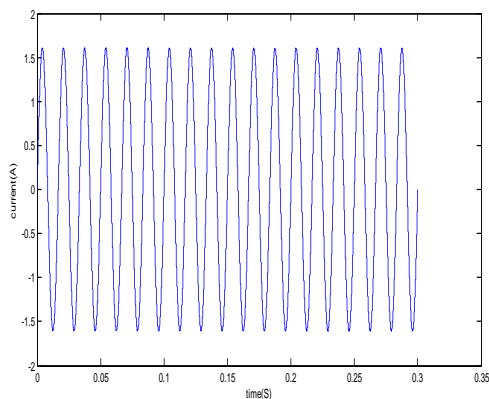


Fig 6(a). Simulation result of r-load current waveform

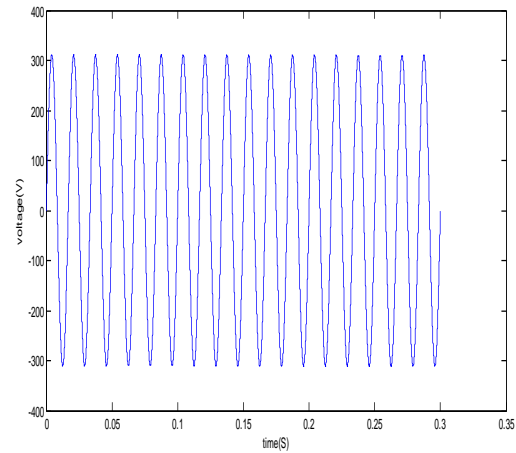


Fig 6(b). Simulation results of r-load voltage waveform

As a result, under the decoupled control of the boost stage, the output voltage u_{OUT} is also well controlled. As to the control variables, since i_L is maintained constant, the waveform of $D_{boostOFF}^*$ will reflect the averaged output current \bar{i}_L while the waveform of D_{buckON}^* will reflect the instantaneous output power. Therefore, $D_{boostOFF}^*$ is expected to be in 50 Hz and has a phase shift of $\arctan(2\pi f_0 R_{Load} C) = 22.5^\circ$ while D_{buckON}^* is expected to be in 100 Hz and greater than zero, both of which can be verified in (b).

(2) Inductive–Resistive Load:

A bipolar, clean ac output larger than the input voltage. This section further examines the system's driving capability for inductive–resistive loads, which represent a large category of industrial loads. In a 1-kVA, 220-V single phase autotransformer is inserted between the resistive load and the inverter. Moreover, because of the saturation characteristics of the core, the equivalent inductance is nonlinear, which is useful to test the system's robustness to different load types. Here, the load resistor is 70 Ω on the secondary side of the autotransformer and the transformer ratio is set to 220:140. The reference for the output voltage is still at 220 Vrms/50 Hz. Fig. 7(a) demonstrates that the output voltage tracks the reference satisfactorily with total harmonic distortion (THD) of only 1.67%. As expected, the load current lags behind the output

voltage and has some distortion due to the saturation of the core. Due to the dead time effect, a larger output voltage distortion (THD = 2.68%) can be observed. Therefore, from the earlier simulations and experiments, it can be concluded that the proposed M-Systems is capable of providing a bipolar, clean ac output larger than the input voltage.

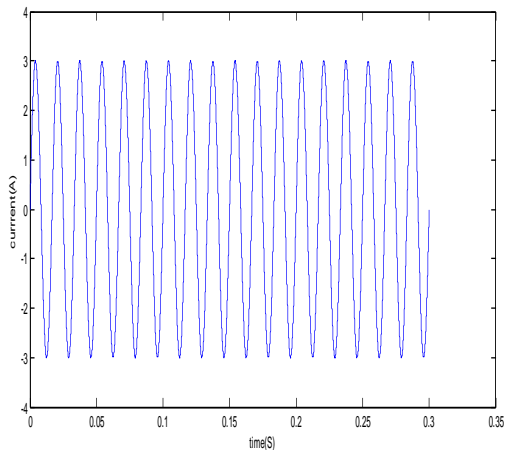


Fig 7(a).simulation results of rl-load current waveform

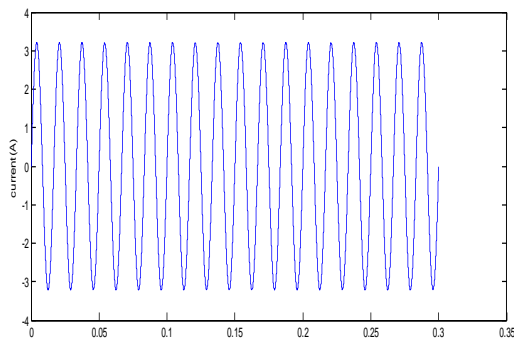


Fig 7(b) simulation results of rl- load voltage waveform

3) Regenerative Load: For some ac motor driving applications and grid-connected applications, such as renewable power systems, energy storage systems, etc., energy needs to be transferred from the load to the battery (or the dc-link capacitor) temporarily or persistently. These loads fall into the category of regenerative load. This section will demonstrate that the proposed system is bidirectional and thus suitable for these applications. The output voltage reference remains

the same while the current reference i_L^* is set to 10 A. In order to simulate a regenerative load, a controlled ac current source with 3.0 A (amplitude), -180° phase angle (with respect to u_{OUT}) is employed. Fig. 8(a) shows that the output voltage can follow the given command and the load current has an opposite phase angle, which indicates that the power flow is reversed.

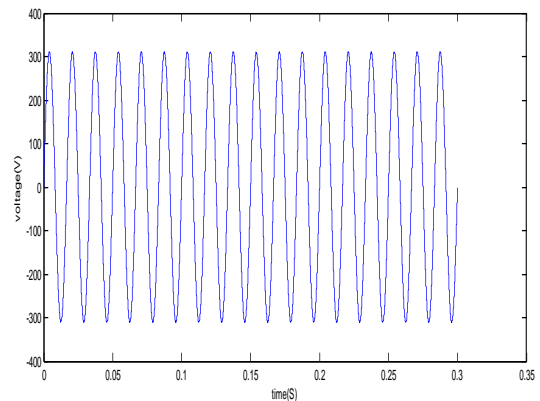


Fig. 8(a) Simulation results of regenerative load current waveform

Fig. 8(b) verifies that, under regenerative condition, $D_{boostOFF}^*$ (proportional to $\overline{i_2}$) has a leading phase larger than 90° and $D_{boostOFF}^*$ (proportional to the instantaneous output power) has a negative average value.

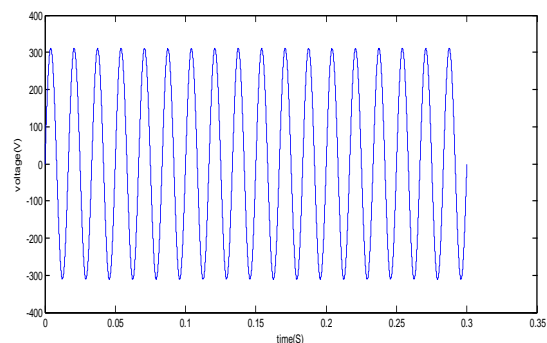


Fig.8(b) simulation results of regenerative load voltage waveform

4) Input Voltage and Load Variations:

This section investigates the robustness of the proposed control to external disturbances. The first disturbance that should be considered is the load variation. For switching power converters, both of the nominal and light load conditions are

concerned. Besides the requirements on a wide load operation range, the converter should also be capable of dealing with sudden load changes. Disturbance that should be noted is the variation of the input voltage, which can easily cause instability of conventional boost inverters. In order to simulate these disturbances, a 100-Hz $\pm 10\%$ square-wave is added to the input voltage and the resistive load suddenly switches from 10 % (968 Ω) to 100 % (96.8 Ω) and then switches back. Simulation results are shown in Fig. 8.

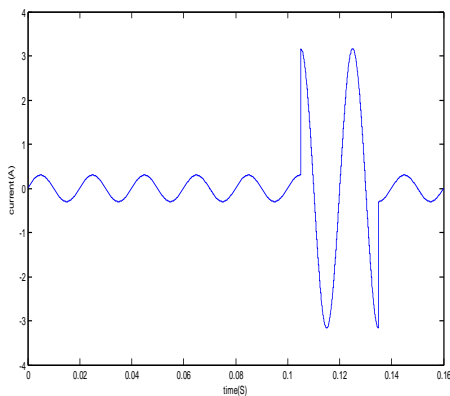


Fig 9(a) Simulation results of input voltage and load variation of current waveform

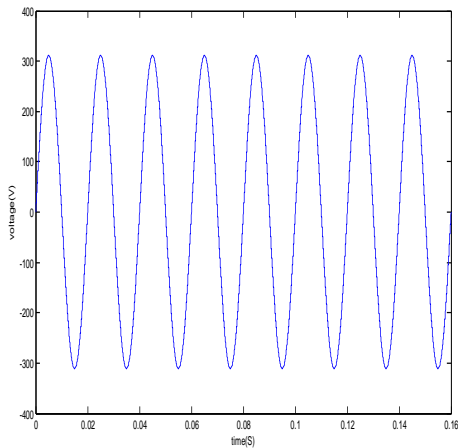


Fig 9(b) Simulation results of input voltage and load variation of voltage waveform

It can be seen that the input voltage disturbance has little effect on the output voltage thanks to the feed forward design (10) of the buck stage. A fast dynamic response to the large load variation can also be observed and there is only a very small variation (about 40 V) of the output voltage during

the transients. This superiority should be attributed to the proposed decoupled control design with additional control freedom.

5) Overload Protection:

This section will demonstrate another merit of the proposed system and its control scheme. That is, without adding extra control modules, the system is equipped with good protection against overload. Initially, a 120- Ω resistor is connected to the inverter. To generate an overload condition, at $t = 0.105$ s another 120- Ω resistor is suddenly connected in parallel. Immediately after the overload occurs, the load current i_{Load} tends to rise rapidly as observed in Fig. 10.

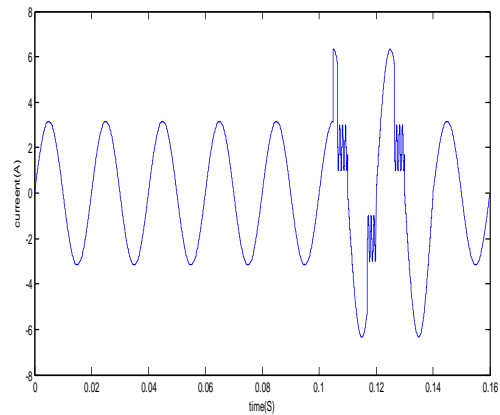


Fig 10(a) Simulation results of overload protection current waveform

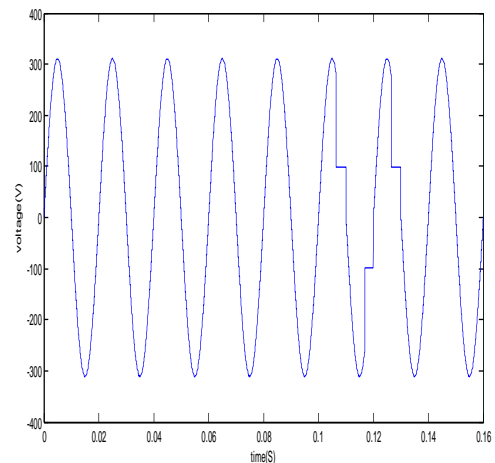


Fig 10(b) Simulation results of over load protection voltage waveform

This requires the boost stage to output more current during a switching cycle. Subsequently, according to

(6), the boost stage controller (i.e., voltage controller) quickly increases $S_{boostOFF}$. As a result, $u_2 = S_{boostOFF} u_{OUT}$ increases simultaneously. However, refer to Fig. 4, when u_2 becomes larger than the maximum output voltage of the buck stage u_{IN} , the inductor current i_L tends to drop.

For the same reason, after $t = 0.11$ s when the output current decreases as the output voltage declines, i_L can quickly restore due to the recovered regulation of buck stage. In sum, during The transients, the output voltage and the inductor current are effectively kept under their rated values, proving the system's excellent current protection. We can eliminate the harmonics present at the load side by using the fuzzy logic controller. We can observe that the harmonics present in the load side will be less when compared to proposed topology. The observing waveform is as shown in above figs.

CONCLUSION

With special consideration on the control superiority, a bidirectional buck-boost cascade inverter is proposed in this paper. It can be seen as the cascade of a buck converter and a boost converter both with bipolar outputs. The switching function model and the averaged model of the system are established and system level analysis reveals that, different from boost-type converters, the proposed converter has one more control freedom, which can be utilized to eliminate the system's nonlinearity, and thus high performance is achieved. Consequently, a decoupled control strategy with feed forward compensation technique is proposed, where main inductor current is regulated by buck stage while the output voltage is controlled by boost stage. By device-level simulations, it is verified that the system possesses the following features: 1) bidirectional operation with bipolar buck/boost output voltage almost free of harmonics; 2) reduced output distortion due to advanced modulation strategy minimizing the dead time effect; 3) reduced volume and weight with only one main energy storage component; 4) simple controller design as only two PI controllers are needed and they can be designed separately; and 5) good steady state and dynamic performance

involving wide operation range, strong robustness to load and input voltage variations, excellent overload protection; 6) Here the two PI controllers are replaced with Fuzzy logic controllers for better performance.

REFERENCES

- [1]. G.-J. Su and L. Tang, "A multiphase, modular, bidirectional, triple-voltage DC-DC converter for hybrid and fuel cell vehicle power," *IEEE Trans. Power Electron.* vol. 23, no. 6, pp. 3035-3046, Nov. 2008.
- [2]. H. Plesko, J. Biela, J. Luomi, and J.W.Kolar, "Novel concepts for integrating the electric drive and auxiliary DC-DC converter for hybrid vehicles," *IEEE Trans. Power Electron.*, vol. 23, no. 6, pp. 3025-3034, Nov. 2008.
- [3]. P. W. Sun, J.-S. Lai, H. Qian, W. S. Yu, C. Smith, and J. Bates, "High efficiency three-phase soft-switching inverter for electric vehicle drives," in *Proc. IEEE Vehicle Power Propulsion Conf. (VPPC)*, 2009, pp. 761-766.
- [4]. F. Blaabjerg, Z. Chen, and S. B. Kjaer, "Power electronics as efficient interface in dispersed power generation systems," *IEEE Trans. Power Electron*, vol. 19, no. 5, pp. 1184-1194, Sep. 2004.
- [5]. Q. Li and P. Wolfs, "A review of the single phase photovoltaic module integrated Converter topologies with three different DC link configurations," *IEEE Trans. Power Electron.*, vol. 23, no. 3, pp. 1320-1333, May 2008.
- [6]. M. Nagao and K. Harada, "Power flow of photovoltaic system using buck-boost PWM power inverter," in *Proc. Int. Conf. Power Electron. Drive Syst.*, May, 1997, vol. 1, pp. 144-149.
- [7]. R. Pena, J. C. Clare, and G. M. Asher, "Doubly fed induction generator using back-to-back PWM converters and its application to variable-speed wind-energy generation," *IEE Proc.—Electr. Power Appl.*, vol. 143, no. 3, pp. 231-241, 1996.
- [8]. M. Mohr and F. W. Fuchs, "Comparison of three phase current source inverters and

- voltage source inverters linked with DC to DC boost converters for fuel cell generation systems," in Proc. Eur. Conf. Power Electron. Appl., 2005, p. 10.
- [9]. R. O. Caceres and I. Barbi, "A boost DC-AC converter: Analysis, design, and experimentation," IEEE Trans. Power Electron., vol. 14, no. 1, pp. 134-141, Jan. 1999.
- [10]. F. Z. Peng, "Z-source inverter," IEEE Trans. Ind. Appl., vol. 39, no. 2, pp. 504-510, Mar./Apr. 2003.
- [11]. F. Z. Peng, M. Shen, and K. Holland, "Application of Z-source inverter for traction drive of fuel cell-battery hybrid electric vehicles," IEEE Trans. Power Electron., vol. 22, no. 3, pp. 1054-1061, May. 2007.
- [12]. M. Shen, A. Joseph, J. Wang, F. Z. Peng, and D. J. Adams, "Comparison of traditional inverters and Z-source inverter," in Proc. IEEE Power Electron. Spec. Conf. (PESC), 2005, pp. 1692-1698.
- [13]. B. Farhangi and S. Farhangi, "Comparison of z-source and boost-buck inverter topologies as a single phase transformer-less photovoltaic grid connected power conditioner," in Proc. IEEE Power Electron. Spec. Conf. (PESC), 2006, pp. 16
- [14]. Y. Tang, S. Xie, C. Zhang, and Z. Xu, "Improved Z-source inverter with reduced Z-source capacitor voltage stress and soft-start capability," IEEE Trans. Power Electron., vol. 24, no. 2, pp. 409-415, Feb. 2009.
- [15]. P. C. Loh, D. M. Vilathgamuwa, C. J. Gajanayake, Y. R. Lim, and C.W. Teo, "Transient modeling and analysis of pulse-width modulated z-source inverter," IEEE Trans. Power Electron., vol. 22, no. 2, pp. 498-507, Mar. 2007.
- [16]. P. Sanchis, A. Ursua, E. Gubia, and L. Marroyo, "Buck-boost DC-AC inverter: Proposal for a new control strategy," in Proc. IEEE Power Electron. Spec. Conf. (PESC), 2004, pp. 3994-3998.
- [17]. P. Sanchis, A. Ursua, E. Gubia, and L. Marroyo, "Boost DC-AC inverter: A new control strategy," IEEE Trans. Power Electron., vol. 20, no. 2, pp. 343-353, Mar. 2005.
- [18]. D. Maksimovic and S. Cuk, "Constant-frequency control of quasi-resonant converters," IEEE Trans. Power Electron., vol. 6, no. 1, pp. 141-150, Jan. 1991.
- [19]. F. Caricchi, F. Crescimbin, and A. D. Napoli, "20 kW water-cooled prototype of a buck-boost bidirectional dc-dc converter topology for electrical vehicle motor drives," in Proc. IEEE Appl. Power Electron. Conf. (APEC), 1995, pp. 887-892.
- [20]. F. Caricchi, F. Crescimbin, F. G. Capponi, and L. Solero, "Study of bi-directional buck-boost converter topologies for application in electrical vehicle motor drives," in Proc. IEEE Appl. Power Electron. Conf. (APEC), 1998, pp. 287-293.
- [21]. P. J. Grbovic, F. Gruson, N. Idir, and P. Le Moigne, "Turn-on performance of reverse blocking IGBT (RB IGBT) and optimization using advanced gate driver," IEEE Trans. Power Electron., vol. 25, no. 4, pp. 970-980, Apr. 2010.
- [22]. J. Itoh, I. Sato, A. Odaka, H. Ohguchi, H. Kodatchi, and N. Eguchi, "A novel approach to practical matrix converter motor drive system with reverse blocking IGBT," IEEE Trans. Power Electron., vol. 20, no. 6, pp. 1356-1363, Nov. 2005.
- [23]. M. Takei, T. Naito, and K. Ueno, "Reverse blocking IGBT for matrix converter with ultra-thin wafer technology," IEE Proc.: Circuits, Devices Syst., vol. 151, no. 3, pp. 243-247, Jun. 2004.